

# Low temperature crystallographic data on Kevlar 49 fibres

R. V. IYER

*Materials Science Division, National Aerospace Laboratories, Bangalore 560 017, India*

K. SOORYANARAYANA, T. N. GURU ROW

*Solid State and Structural Chemistry Unit, Indian Institute of Science, Bangalore 560 012, India*

K. VIJAYAN\*

*Materials Science Division, National Aerospace Laboratories, Bangalore 560 017, India*

*E-mail: kavi@css.cmmacs.ernet.in*

Using X-ray diffraction data, the behaviour of Kevlar 49 fibres at low temperatures, up to  $-100^{\circ}\text{C}$ , has been analysed. During cooling, the basal plane of the monoclinic unit cell shrinks whereas the  $c$ - (unique, chain axis) length is not significantly affected. In contrast, in the return heating cycle to ambient temperature, the basal plane expands and contraction occurs along the chain direction. The unit cell registers a reduction in volume in both the cooling and heating cycles. Conspicuously, after a cycle of cooling and heating, the unit cell does not return to its initial volume. © 2003 Kluwer Academic Publishers

## 1. Introduction

Kevlar is a high strength, high modulus, light weight aramid fibre commercialised by DuPont Inc., USA. The wide range of applications of Kevlar fibres includes use in deep sea environment and also high up in space [1] where the fibres or components made of the fibres can get exposed to temperatures ( $T$ ) less than the ambient temperature of  $\sim 24^{\circ}\text{C}$ . Although extensive work has been carried out on the high temperature behaviour of Kevlar fibres [2–12], very little is known about Kevlar at low temperatures. Yang [13], in a review on Kevlar fibres, mentions that when the fibres are exposed to temperatures as low as  $-196^{\circ}\text{C}$ , no embrittlement or degradation occurs. Jackson et al. [14] have investigated the dynamics of the amide bond of PPTA in the temperature range  $-184$  to  $228^{\circ}\text{C}$  using one dimensional quadrupole echo  $^2\text{H}$  NMR method. In a later study, Schaefer and English [15] have elucidated the dynamics of the  $p$ -phenylene diamine rings of PPTA in the temperature range  $-119$  to  $75^{\circ}\text{C}$  using two dimensional exchange solid state  $^2\text{H}$  NMR spectroscopy. Conspicuously, none of these earlier studies at low temperatures concern the crystallographic characteristics. This paper reports the details of the first investigation on the crystal structural characteristics of Kevlar 49 fibres at low temperatures, derived by X-ray diffraction methods, using an *in situ* cooling/heating arrangement.

## 2. Experimental details

The samples used were Kevlar 49 fibres commercialised by DuPont Inc., USA X-ray diffraction patterns were recorded using a STOE/STADI-P computer

controlled powder diffractometer, in the transmission geometry. Germanium monochromated  $\text{CuK}\alpha 1$  radiation was employed. A curved position sensitive detector was used. The patterns were recorded at the following temperatures in the sequence given below:

Room  $\Rightarrow 0^{\circ}\text{C} \Rightarrow -50^{\circ}\text{C} \Rightarrow -100^{\circ}\text{C} \Rightarrow$  Room

temperature temperature  
( $24^{\circ}\text{C}$ )(RT1) ( $24^{\circ}\text{C}$ )(RT2)

To distinguish between the two room temperature patterns, the ambient temperature prior to cooling is referred to as RT1 and that reached after excursion to the chosen lowermost temperature of  $-100^{\circ}\text{C}$  is referred to as RT2. To reach  $T$ 's  $< 24^{\circ}\text{C}$  a programmable Oxford cryogenic system with liquid nitrogen as the cooling agent was used. The rate of cooling was  $-2^{\circ}\text{C}/\text{min}$ . The sample was cooled by a spray of liquid nitrogen from a nozzle. Care was taken to ensure that the fibres were as close as possible to the nozzle tip and at the same time secure enough so that they did not get displaced during the recording of the X-ray diffraction patterns. After recording the X-ray diffraction patterns at  $-100^{\circ}\text{C}$ , the cryostat was switched off and the fibres were allowed to return to room temperature in an uncontrolled heating process. It took about an hour to warm up from  $-100^{\circ}\text{C}$  to RT2.

In these experiments, after reaching the chosen temperatures, 5 minutes were allowed for stabilisation. While recording the diffraction patterns, the temperature remained stable upto an accuracy of  $\pm 0.5^{\circ}\text{C}$ . Both equatorial and meridional patterns were recorded in

\* Author to whom all correspondence should be addressed.



the  $2\theta$  range  $8-72^\circ$  using tautly held bundles of fibres  $\sim 0.3$  mm thick. As the diffractometer circle was horizontal, the fibres were mounted vertically to record the equatorial reflections and then rotated by  $90^\circ$  to the horizontal position to record the meridional reflections. The equatorial and the meridional patterns included the reflections (110), (200), (310) and (002), (004), (006) respectively. At each of the chosen temperatures the fibre was exposed for  $\sim 1$  h.

The parameters  $2\theta_{\max}$ , half width  $\omega$  and the integrated intensity  $I$  of individual reflections were derived by fitting the diffractometer menu driven Lorentzian<sup>2</sup> function to the observed diffraction profiles. As is well known, values of the estimated standard deviations of

these parameters are also calculated by the software package. The unit cell constants  $a$  and  $b$  were estimated from the equatorial reflections (200) and (110) respectively. As the reflection (310) was comparatively weak it was not included in the calculations. Among the meridional reflections, (002) was quite weak and could not be used reliably. The higher angle reflection (006) was slightly asymmetric and hence the subsequent profile fitting used to derive the profile parameters had a comparatively high reliability factor. Hence, the unit cell constant  $c$  was determined using the reflection (004) only. Values of residual crystallinity,  $K$ , were estimated from the ratio  $I/I_0$  where  $I_0$  and  $I$  correspond to the integrated intensities at RT and at any other temperature respectively.

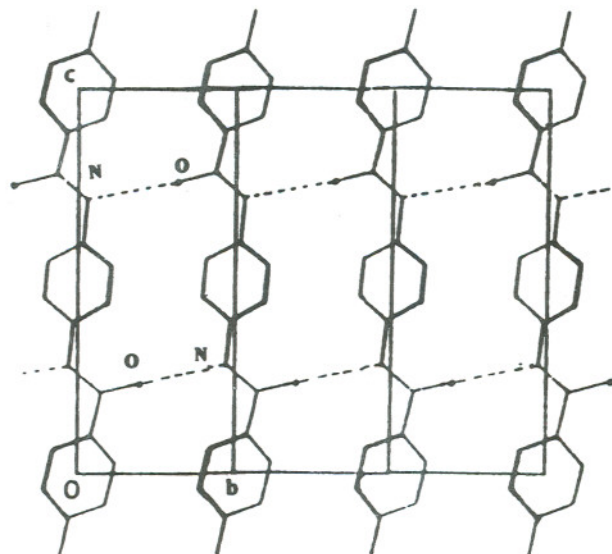


Figure 1 Molecular arrangement in the crystallographic  $bc$ -plane of the unit cell. The dashed lines represent the inter chain hydrogen bonds.

### 3. Results and discussion

Kevlar crystallises in the monoclinic space group Pn or  $P2_1/n$  [16, 17]. In the crystal structure poly (p-phenylene terephthalamide) or PPTA (Fig. 1) chains of which Kevlar is made of [18], are fully extended in an all *trans* conformation and are oriented along the crystallographic  $c$ -direction. (unique axis). Adjacent chains along the  $b$ -direction interact by the formation of inter chain  $NH \dots O$  hydrogen bonds. The layers thus stabilised by hydrogen bonds are stacked periodically along the crystallographic  $a$ -direction.

Figs 2 and 3 present the equatorial and the meridional diffraction patterns respectively. As a typical example, in each category, only one low temperature pattern has been included. The diffraction patterns at ambient and low temperatures are remarkably similar thereby showing that the crystal structure is basically unaffected by exposure to the chosen low temperatures. Examination of the profile characteristics, however, indicate

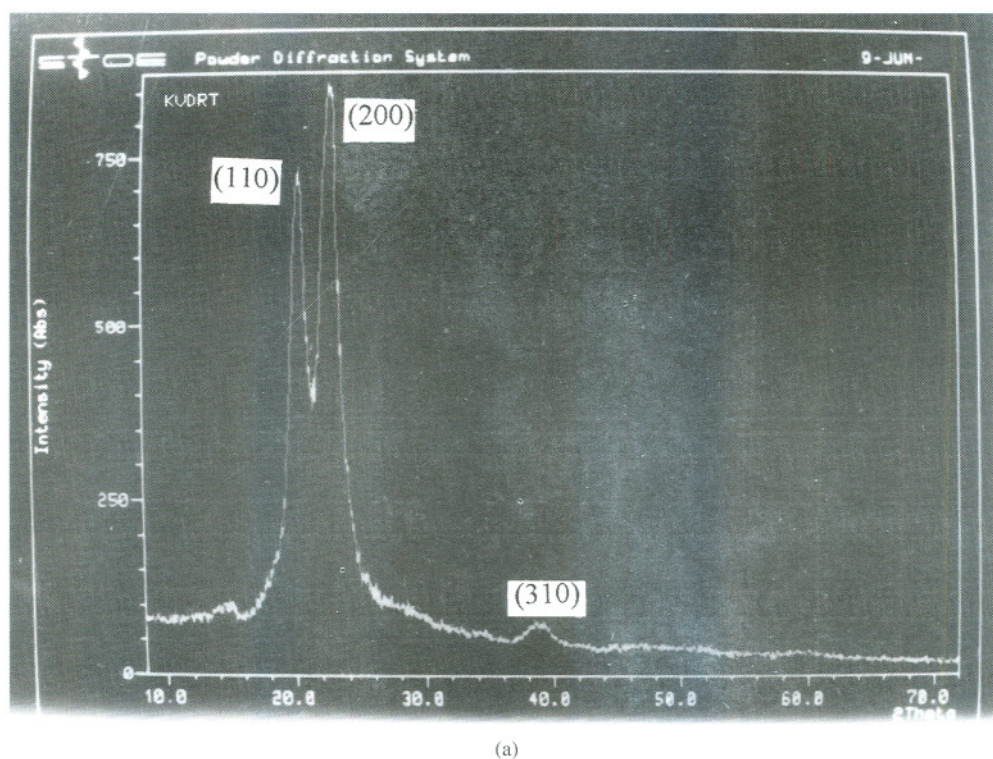
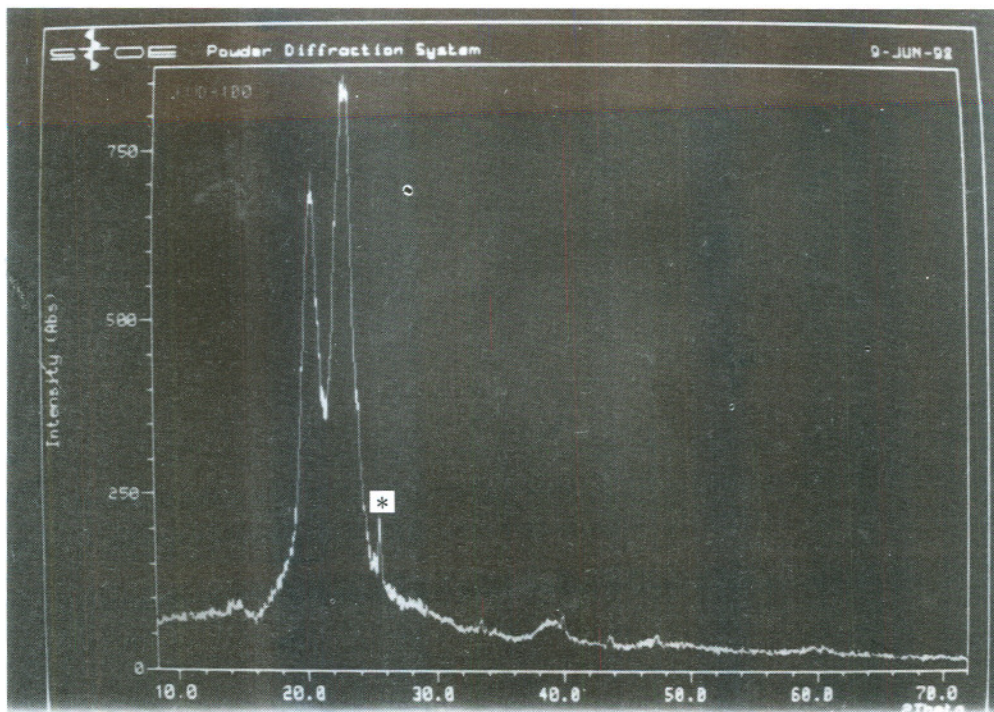
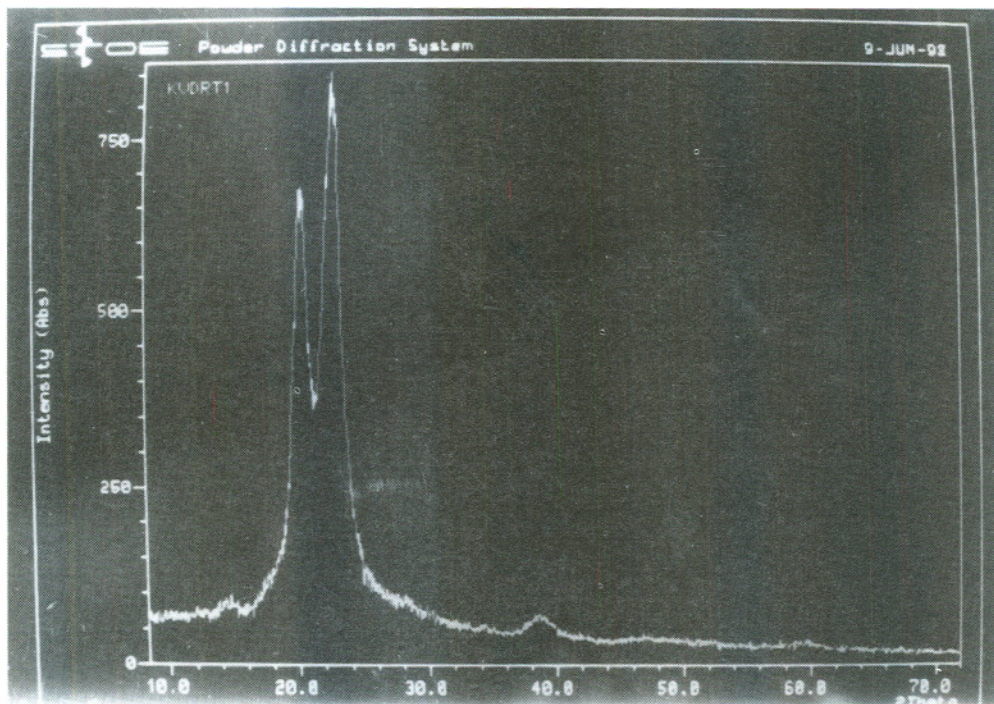


Figure 2 Equatorial diffraction profiles from fibres (a) prior to cooling (RT1) (b) At  $-100^\circ\text{C}$  and (c) At RT2. Where \* is Ice peak. (Continued.)





(b)



(c)

Figure 2 (Continued).

interesting features, viz., (i) during heating as well as cooling, the unit cell manifests an anisotropic dimensional change and (ii) in the return, heating cycle the unit cell does not return to its initial dimensions. Details of these observations are presented below.

### 3.1. Basal plane dimensions

With lowering of temperature, the  $2\theta_{\max}$  values of the equatorial reflections exhibit a progressive shift towards higher angles. Most of the observed shifts ( $\Delta$ 's) in the  $2\theta_{\max}$  values, though small, are statistically significant, with  $|\Delta|/\sigma > 3$ . Here  $\sigma$  is the standard deviation of the  $\Delta$  value. Table I presents the percentage variations

in the unit cell dimensions. Here,  $a_0$ ,  $b_0$  and  $c_0$  correspond to the parameters at RT1. With the lowering of temperature from RT1 to  $-100^\circ\text{C}$ , both  $a$ - and  $b$ -values decrease progressively. At  $T = -100^\circ\text{C}$ , the reductions are  $\sim 0.7$  and  $0.1\%$  respectively. The difference in the magnitudes of the reductions in the  $a$ - and  $b$ -values is indeed conspicuous. It must be mentioned that similar preferential change in the  $a$ -value has been observed in Kevlar 49 fibres exposed to  $T$ 's up to  $500^\circ\text{C}$  also [8, 9, 12]. It appears therefore that in the basal plane, the  $a$ -dimension is readily affected by changes in temperature, be it high or low, than the  $b$ -dimension. The preferential sensitivity of the  $a$ -length may be associated



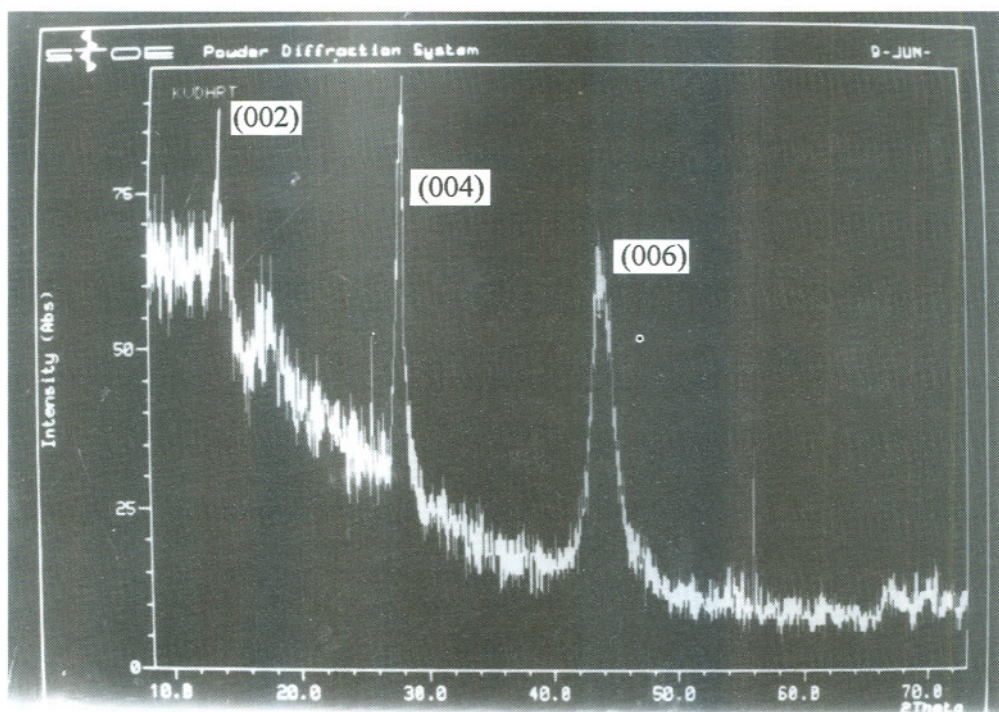
TABLE I Percentages variations in the unit cell dimensions

Temperature (°C)	$(\Delta a/a_0)100$	$(\Delta b/b_0)100$	$(\Delta c/c_0)100$	$(\Delta A/A_0)100$	$(\Delta V/V_0)100$
RT1	—	—	—	—	—
0	-0.123	0.094	0.002	-0.030	-0.027
-50	-0.401	-0.059	0.006	-0.459	-0.453
-100	-0.698	-0.117	-0.061	-0.815	-0.877
RT2	0.236	0.249	-2.537	0.486	-2.064

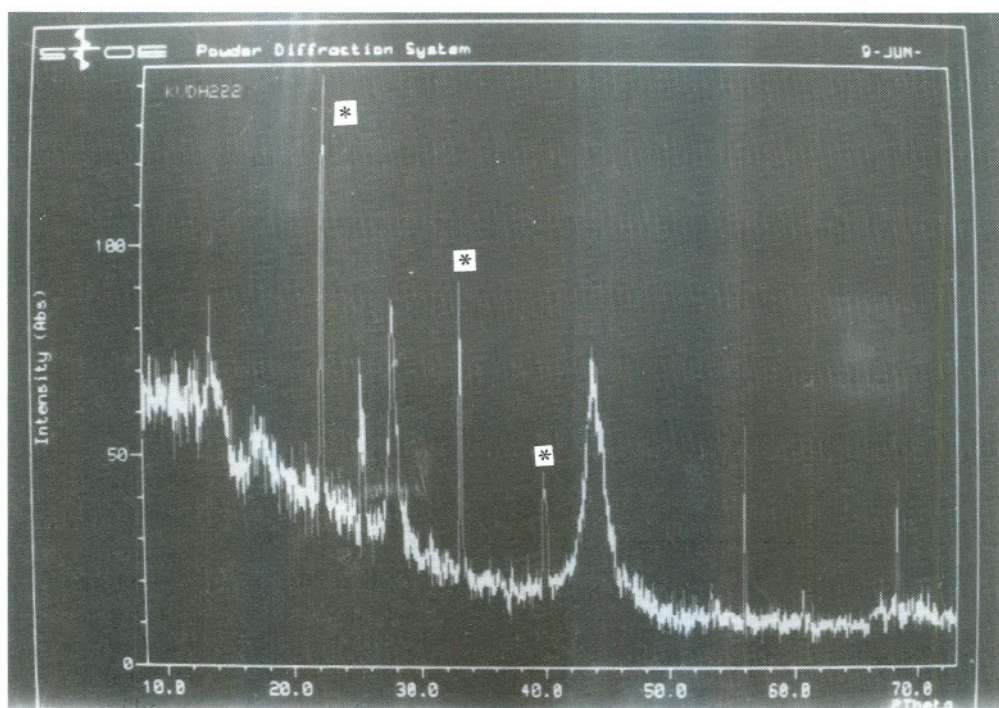
The  $\Delta$ 's in columns 2-6 are defined as  $(\text{Low temperature}/\text{RT2}) - (\text{RT1})$ .

The unit cell dimensions at RT1 are indicated by the subscript 0.

The increase in the basal plane area in the heating cycle from  $-100^\circ\text{C}$  to RT2 is  $\sim 1.3\%$  (Not listed in the table).



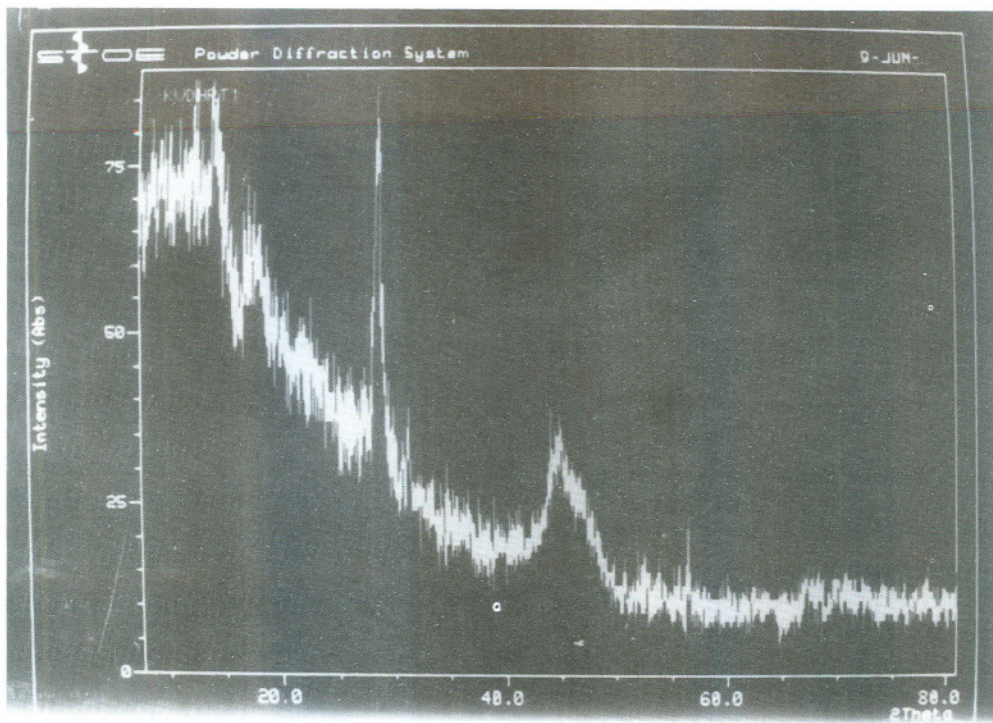
(a)



(b)

Figure 3 Meridional diffraction profiles from fibres: (a) prior to cooling (RT1) (b) at  $-50^\circ\text{C}$  and (c) at RT2. Where \* is Ice peak. (Continued.)





(c)

Figure 3 (Continued).

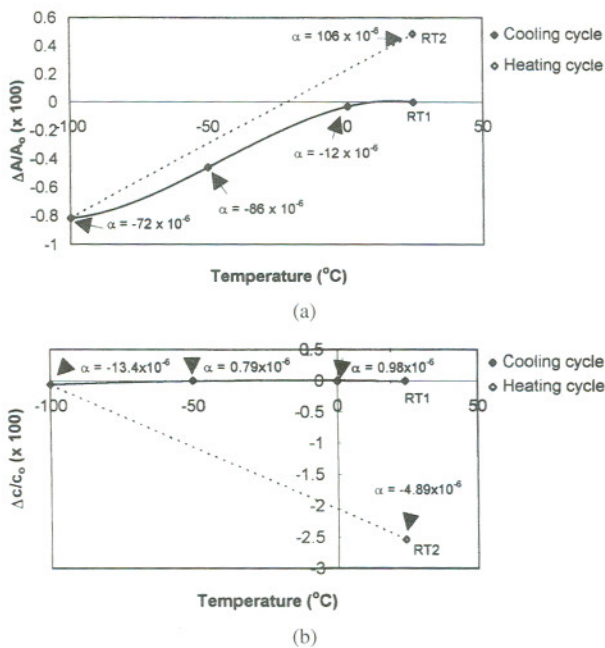


Figure 4 Percentage variation in the (a) basal plane area, (b) axial length for the cooling and heating cycles respectively. Values of  $\alpha$  ( $1/^\circ\text{C}$ ), calculated using adjacent data points, have also been included.

with the presence of van der Waal's interactions along the crystallographic  $a$ -direction [16].

The shrinkage in the basal plane area,  $A$  is depicted in Fig. 4a. At  $-100^\circ\text{C}$ , the reduction is  $\sim -0.8\%$ . In the return, heating cycle from  $-100^\circ\text{C}$  to RT2, the basal plane, however, enlarges. These observations are not very surprising because most materials exhibit shrinkage during cooling and expansion during heating and the basal plane of Kevlar 49 fibres exhibits this conventional behaviour.

The interesting feature, however, concerns the relative dimensions of the basal plane at RT1 and RT2

respectively. Although both refer to the ambient temperature of  $\sim 24^\circ\text{C}$ , the dimensions at RT1 and RT2 are not the same. As shown in Fig. 4a in the return, heating cycle from  $-100^\circ\text{C}$  to RT2, the magnitude of the expansion is much more than the shrinkage introduced during cooling from RT1 to  $-100^\circ\text{C}$ . Thus, the result of cooling from RT1 to  $-100^\circ\text{C}$  and returning to RT2, leaves the basal plane with a 0.5% expansion from the initial area.

In Fig. 4a the coefficients of negative thermal expansion,  $\alpha_A$ , of the basal plane area for adjacent temperature ranges have been marked. The variation of  $\alpha_A$  with  $T$  is not linear. For the entire range of cooling from RT1 to  $-100^\circ\text{C}$ , the value of  $\alpha_A$  is  $-65.7 \times 10^{-6}/^\circ\text{C}$ . In contrast, the coefficient of thermal expansion corresponding to heating from  $-100^\circ\text{C}$  to RT2 is  $105.8 \times 10^{-6}/^\circ\text{C}$  and is  $\sim 1.6$  times the coefficient of contraction observed during cooling through the same temperature range. It must be pointed out that in the present study, the cooling and heating rates were not identical. Although cooling upto  $-100^\circ\text{C}$  was at the rate of  $2^\circ\text{C}/\text{min}$ , heating from  $-100^\circ\text{C}$  to RT2 was uncontrolled. Possible contribution from the difference in cooling and heating rates to the observed differences in the  $\alpha_A$ 's during heating and cooling, cannot be ruled out.

### 3.2. Axial dimension

The behaviour of the axial dimension during cooling is very different from that of the basal plane. The striking feature is that at  $T$ 's  $< 24^\circ\text{C}$ , the observed shifts in the  $2\theta_{\text{max}}$  values of the meridional reflections are not statistically significant, the  $|\Delta|/\sigma$  values being  $< 1$ . As seen from Fig. 1, in the crystal structure of Kevlar, the  $c$ -length of the unit cell represents the end-to-end length of a PPTA monomer which has an all *trans* fully extended conformation [16]. Absence of significant



shifts in the  $2\theta_{\max}$  values suggests that exposures to temperatures up to  $-100^{\circ}\text{C}$ , do not introduce significant changes in the initial molecular conformation. Fig. 4b presents the percentage variation in the  $c$ -length which, for reasons mentioned above are not considered statistically significant.

It has been reported that Kevlar 49 fibres exhibit a macro axial contraction during heating [19, 20]. The recent high temperature studies of Jain and Vijayan [19] showed that similar to the macro behaviour of the fibre, the crystallographic unit cell also manifests an axial contraction during heating. Thus, the negative axial expansion characteristic of the molecules in the crystallographic unit cell and also of the entire fibre, during heating, has been unambiguously established in the past. The near invariance of the  $c$ -length during cooling, observed in the present study suggests that although heating introduces contraction, cooling causes no significant changes in dimension.

Unlike in the case of data corresponding to cooling the  $|\Delta|/\sigma$  value for the shift in the  $2\theta_{\max}$  value introduced during heating from  $-100^{\circ}\text{C}$  to RT2 is  $\sim 52$  and this shift is indeed statistically reliable. Fig. 4b depicts the reduction of  $\sim 2.5\%$  in the  $c$ -length during the return heating cycle from  $-100^{\circ}\text{C}$  to RT2. The coefficient of negative thermal expansion,  $\alpha_A$ , corresponding to the observed shrinkage has also been marked in Fig. 4b.

As in the case of the basal plane dimensions, the  $c$ -value at RT2 is very different from the starting value at RT1. The striking difference, however, concerns the directions of change. Whereas the basal plane expands during heating, the axial length contracts, leading to the following inequalities

$$\text{Basal plane: } (a, b)_{\text{RT1}} < (a, b)_{\text{RT2}}$$

$$\text{Axial dimension: } (c)_{\text{RT1}} > (c)_{\text{RT2}}$$

### 3.3. Unit cell volume, $V$

Fig. 5 presents the percentage variation in the unit cell volume. It is seen that in the cooling cycle the unit cell contracts, with the major contribution to the shrinkage arising from the reduction in the basal plane dimensions. Interestingly, in the heating cycle also, the unit cell contracts, despite an increase in the basal plane area by  $\sim 1.3\%$ . The principal contributor to the reduction in volume is the shrinkage of the  $c$ -axial dimension by

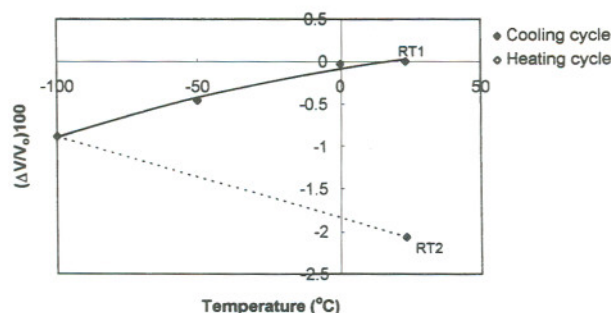


Figure 5 Percentage variation in the unit cell volume for the cooling and heating cycles respectively.

$\sim 2.5\%$  which is significantly more than the increase in the basal plane area. Thus, after undergoing a cycle comprising of both cooling and heating of the type described above, Kevlar 49 fibres are characterised by a crystallographic unit cell smaller than the initial one. It must be pointed out that similar data regarding the effect of cyclic cooling and heating on the macro behaviour of the fibre are not available in literature.

The negative axial expansion of Kevlar 49 fibres has been a cause of concern to users of Kevlar fibre reinforced composites, at elevated temperatures. In a composite, if there is anisotropic shrinkage in the volume of the fibre at elevated temperatures, the properties of the components made of the composite can deviate from the initial values and thus affect their anticipated performance. The present study suggests that another similar cause of concern may arise from cyclic cooling and heating. If the behaviour of the unit cell which has emerged from the present study could be extrapolated to the macro behaviour of the fibre, it is likely that when components made of Kevlar 49 fibres get exposed to low temperature and then brought back to ambient conditions, the fibre fraction of the composite would have suffered a residual, reduction in volume which in turn can affect the properties and performance of the composite.

### 3.4. Half width, $\omega$

As is well known, the half widths of X-ray reflections are related to the crystallite size and microstrain. In the case of Kevlar fibres, changes in half width values of both the equatorial and meridional reflections during heating as well as cooling were statistically not significant. Neither the crystallite size nor the lattice strains of Kevlar 49 fibres thus appear to be sensitive to exposures to low temperatures.

### 3.5. Crystallinity

It is well known that the crystallinity of a diffracting material affects the total intensity distribution in the X-ray diffraction pattern [22]. The crystallinity of a fibre, in turn, is closely related to its tensile modulus. Relative changes in the crystallinity values can be identified from a comparison of the integrated intensities, estimated under identical experimental conditions. Based on the correlation between  $I$  and crystallinity, the temperature induced variations in the residual crystallinity values of Kevlar 49 fibres have been derived (Fig. 6). Here, the integrated intensities of the equatorial patterns have been used. In the cooling cycle from RT1 to  $-100^{\circ}\text{C}$ , the crystallinity increases by  $\sim 1.6\%$ . In contrast, in the heating cycle the crystallinity reduces by  $\sim 8\%$ . This decrease is similar to the behaviour of fibres heated above  $24^{\circ}\text{C}$  [8, 10]. The correlation between crystallinity and tensile properties suggests that the tensile modulus of Kevlar 49 fibres exposed to low temperatures may be expected to be adversely affected. Details of the experiments which establish the changes in the tensile modulus of Kevlar 49 fibres exposed to low temperatures will be presented elsewhere.



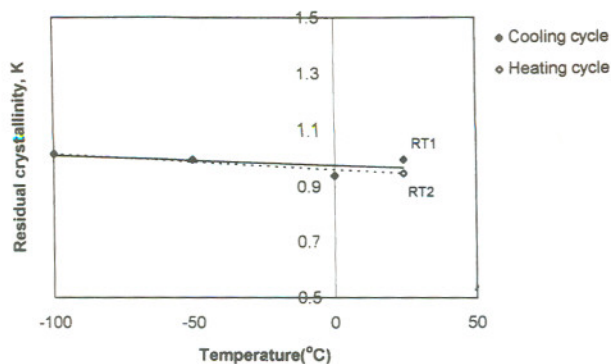


Figure 6 Variation in the residual crystallinity in the cooling and heating cycles respectively.

#### 4. Conclusion

Exposures of Kevlar 49 fibres to low temperatures upto  $-100^{\circ}\text{C}$  and subsequent heating to ambient temperature of  $\sim 24^{\circ}\text{C}$ , both introduce anisotropic dimensional changes in the crystallographic unit cell. In the cooling cycle, the basal plane of the monoclinic cell shrinks and the axial dimension which corresponds to the repeat unit of the PPTA chain does not register any significant change. In contrast, in the heating cycle, the basal plane expands and the axial dimension shrinks. Interestingly, the unit cell registers a reduction in volume in both the cooling and the heating cycles. After the cooling and heating cycles, the unit cell does not return to its initial dimensions. Crystallinity values suggest a reduction in the tensile modulus.

#### Acknowledgement

R. V. Iyer wishes to thank NalTech, Bangalore for providing him with financial assistance. The authors thank Dr. T. S. Prahlad, Director, National Aerospace laboratories for the support.

#### References

1. R. E. WILFONG and J. ZIMMERMAN, *J. Appl. Polym. Symp.* **31** (1977) 1.
2. A. M. HINDELEH and M. SH. ABDO, *Polymer* **30** (1989) 218.
3. H. V. PARIMALA and K. VIJAYAN, *J. Mater. Sci. Lett.* **12** (1993) 99.
4. R. V. IYER and K. VIJAYAN, in "Polymer Science Recent Advances," Vol. 1, edited by I. S. Bhardwaj (Allied Publishers Ltd., New Delhi, 1994) p. 362.
5. *Idem.*, in "Macromolecules New Frontiers," Vol. 2, edited by K. S. V. Srinivasan (Allied Publishers Ltd, New Delhi, 1998 p. 847.
6. *Idem.*, *Curr. Sci.* **75** (1998) 946.
7. *Idem.*, *J. Mater. Sci.* **35** (2000) 573.
8. *Idem.*, *Bull. Mater. Sci.* **22** (1999) 1013.
9. K. VIJAYAN, *Metals, Materials and Processes* **12** (2000) 259.
10. M. SHUBHA, M. Phil. Dissertation, Mangalore University, India (1989).
11. H. V. PARIMALA, M. Phil. Dissertation, Mangalore University, India (1991).
12. R. V. IYER, Ph. D. Thesis, Bangalore University, India (1999).
13. H. H. YANG, in "Kevlar Aramid Fibre" (John Wiley & Sons, Chichester, 1993).
14. C. L. JACKSON, R. J. SCHADI, K. H. GARDNER, D. B. CHASE, S. R. ALLEN, V. GABARA and A. D. ENGLISH, *Polymer* **35** (1994) 1123.
15. D. J. SCHAEFER and A. D. ENGLISH, *ibid* **36** (1995) 2517.
16. M. G. NORTHOLT, *Eur. Polym. J.* **10** (1974) 799.
17. K. TASHIRO, M. KOBAYASHI and H. TADOKORO, *Macromolecules* **10** (1977) 413.
18. S. ROJSTACZER, D. COHN and G. MACROM, *J. Mater. Sci. Lett.* **3** (1984) 1028; **4** (1985) 1233.
19. A. JAIN and K. VIJAYAN, *Curr. Sci.* **78** (2000) 331.
20. J. H. WAKELIN and R. MEREDITH, *Text. Progr.* **7**(4) (1975).
21. Kevlar 49 Data Manual, E. I. DuPont de Nemours & Co.
22. H. S. VIRGIN and E. J. CRYSTAL, *J. Appl. Phys.* **30** (1959) 1654.

Received 5 June 2001

and accepted 9 September 2002